Supporting Information

Piezoelectricity Enhancement of Nanogenerators Based on PDMS and $ZnSnO_3$ Nanowires through Micro-structuration

Ana Rovisco,[‡,§] Andreia dos Santos,[‡,§] Tobias Cramer,[⊥] Jorge Martins,[§] Rita Branquinho,[§] Hugo Águas,[§] Beatrice Fraboni,[⊥] Elvira Fortunato,[§] Rodrigo Martins,[§] Rui Igreja[,§] and Pedro Barquinha*[,§]*

[§] i3N/CENIMAT, Department of Materials Science, Faculty of Science and Technology, Universidade NOVA de Lisboa and CEMOP/UNINOVA, Campus de Caparica, 2829-516 Caparica, Portugal.

[⊥] Department of Physics and Astronomy, University of Bologna, Viale Berti Pichat 6/2, 40127 Bologna, Italy.

* E-mail: rni@fct.unl.pt, pmcb@fct.unl.pt.

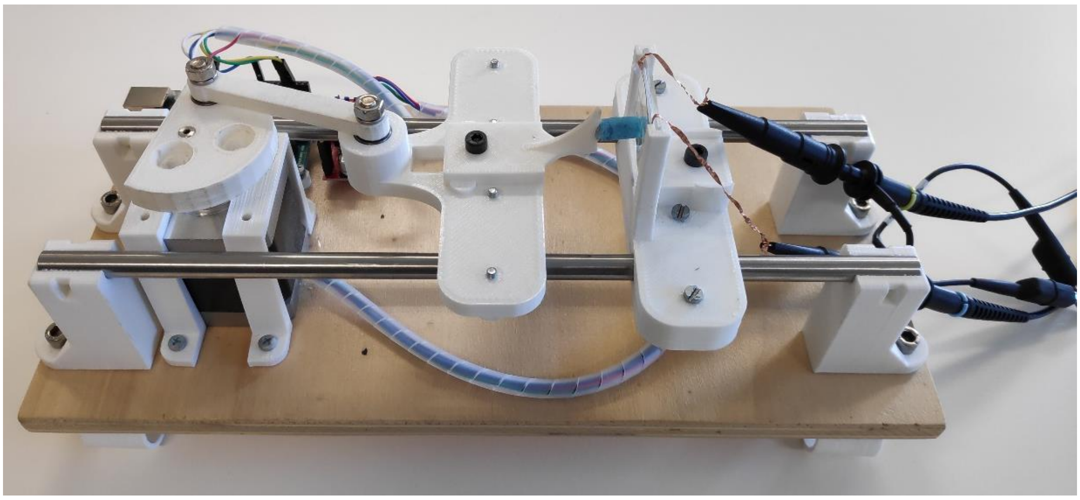

Figure S1. Photograph image of the home-made machine used for the measurements.

Note S1. ZnO nanowires synthesis

For ZnO nanostructures synthesis zinc acetate dihydrate ($Zn(CH_3COO)_2 \cdot 2H_2O$; 0.45 M) from Sigma-Aldrich was dissolved in deionized water and sodium hydroxide (NaOH; 8 M) from Eka was added (**solution A**). In order to stabilize the nanostructures, to prevent the formation of agglomerates and to help with the nanorods length growth, a surfactant, sodium lauryl sulfate ($NaC_{12}H_{25}SO_4$) from Scharlau was used, being also dissolved in deionized water with a molar concentration of 1.04 mM (**solution B**). The final solution was achieved mixing 2 mL of solution A, 5 mL of solution B and 10 mL of deionized water. The mixture was then transferred into a Teflon vessel (with a capacity of 50 mL). Three vessels were loaded at the same time into a CEM Mars One microwave, with a capacity for 12 vessels, being the microwave parameters set as 110 °C of temperature, 600 W of power, 7 min until reaching the set temperature and then 40 min of synthesis. The resultant precipitate of nanowires' syntheses was centrifuged at 4000 rpm and washed several times with deionized water and isopropyl alcohol, alternately. The nanostructures were finally left drying at room temperature for at least 72 h.[1]

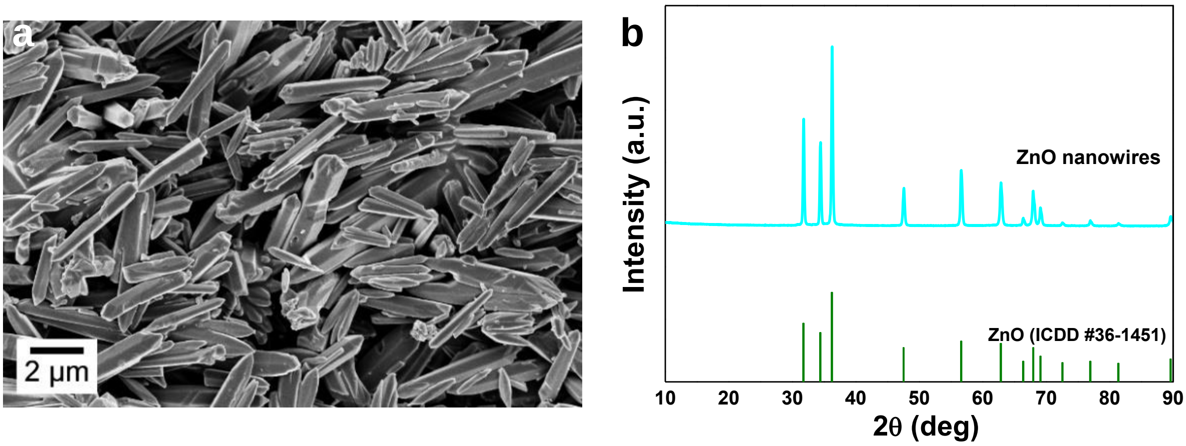

Figure S2. Characterization of ZnO nanowires. (a) SEM image. (b) XRD pattern. The identification was following ICDD card #36-1451.

Table S1. Piezoelectric coefficient of some of 1D piezoelectric nanostructures produced by hydrothermal synthesis.

Material	**d_{33} (pm/V)**	**Ref.**
$ZnSnO_3$	23.0 ± 4	This work
BNT	15.0	[2]
$KNbO_3$	10.8	[3]
SbSI	12.0	[4]
$Na_6(W_6O_{19})(SeO_3)_2$	12.0	[5]
$NaNbO_3$	4.0	[6]
$BaTiO_3$	31.1	[7]
$LiNbO_3$	25.0	[8]
$KNbO_3$	11.6	[9]

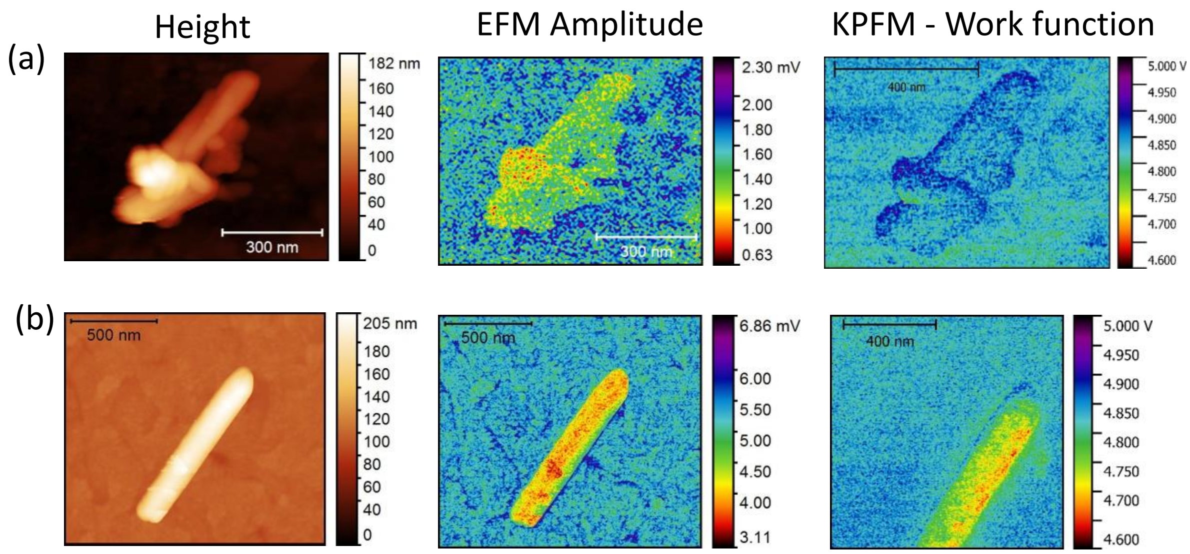

Figure S3. Electrostatic force microscopy of $ZnSnO_3$ (a) and ZnO (b) nanowires on ITO substrate. The amplitude in electrostatic force modulation (EFM) is reduced for both kinds of nanowires in comparison to the ITO surface. At the same time the local surface potential is not altered for $ZnSnO_3$ and slightly modified for ZnO leading to a local work function of 4.7 eV. This value is in agreement with literature data found on vacancy doped ZnO. The reduction in EFM amplitude rules out the presence of electrostatic surface charges.

	Aligned	Misaligned

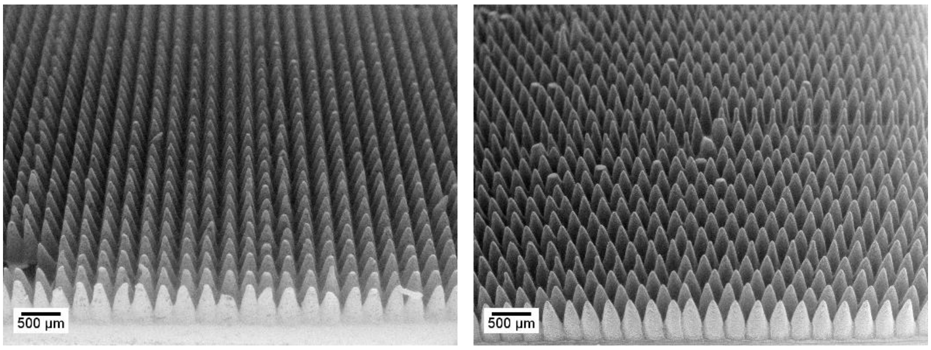

Gap	0 µm	0 µm
Height	360 µm	300 µm
Diameter	220 µm	230 µm

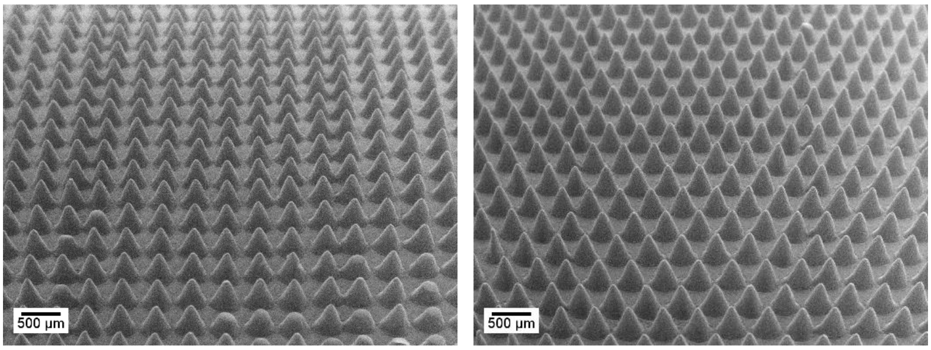

Gap	90 µm	60 µm
Height	380 µm	400 µm
Diameter	300 µm	330 µm

Figure S4. SEM images of micro-structured PDMS films.

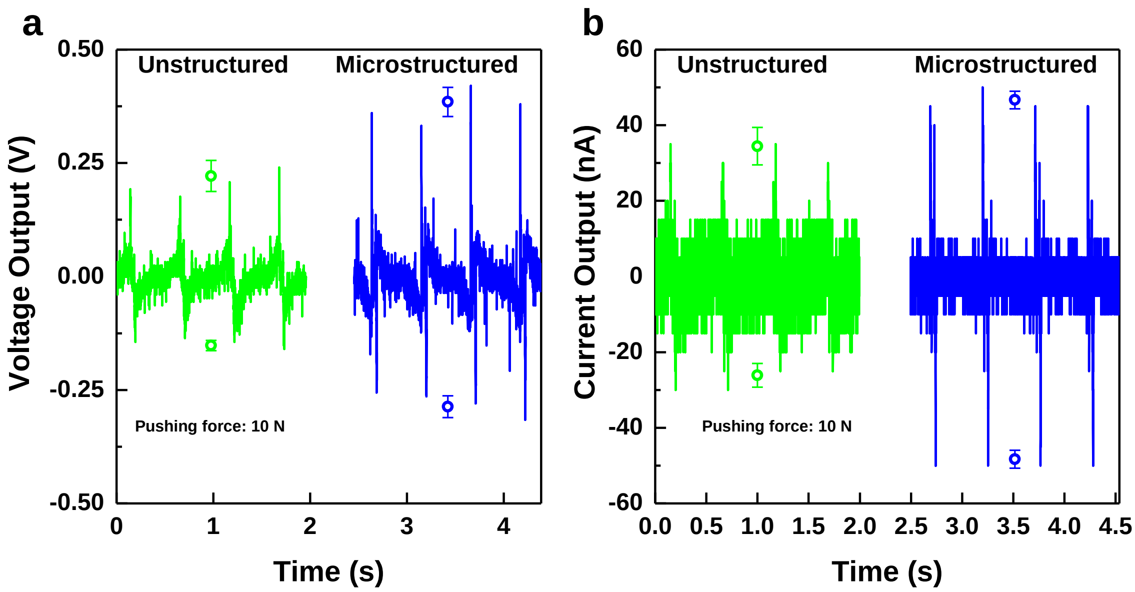

Figure S5. Output voltage (a) and current (b) signals of unstructured (green) and micro-structured (with aligned micro-cones with a gap between cones < 100 μm, blue) PDMS films.

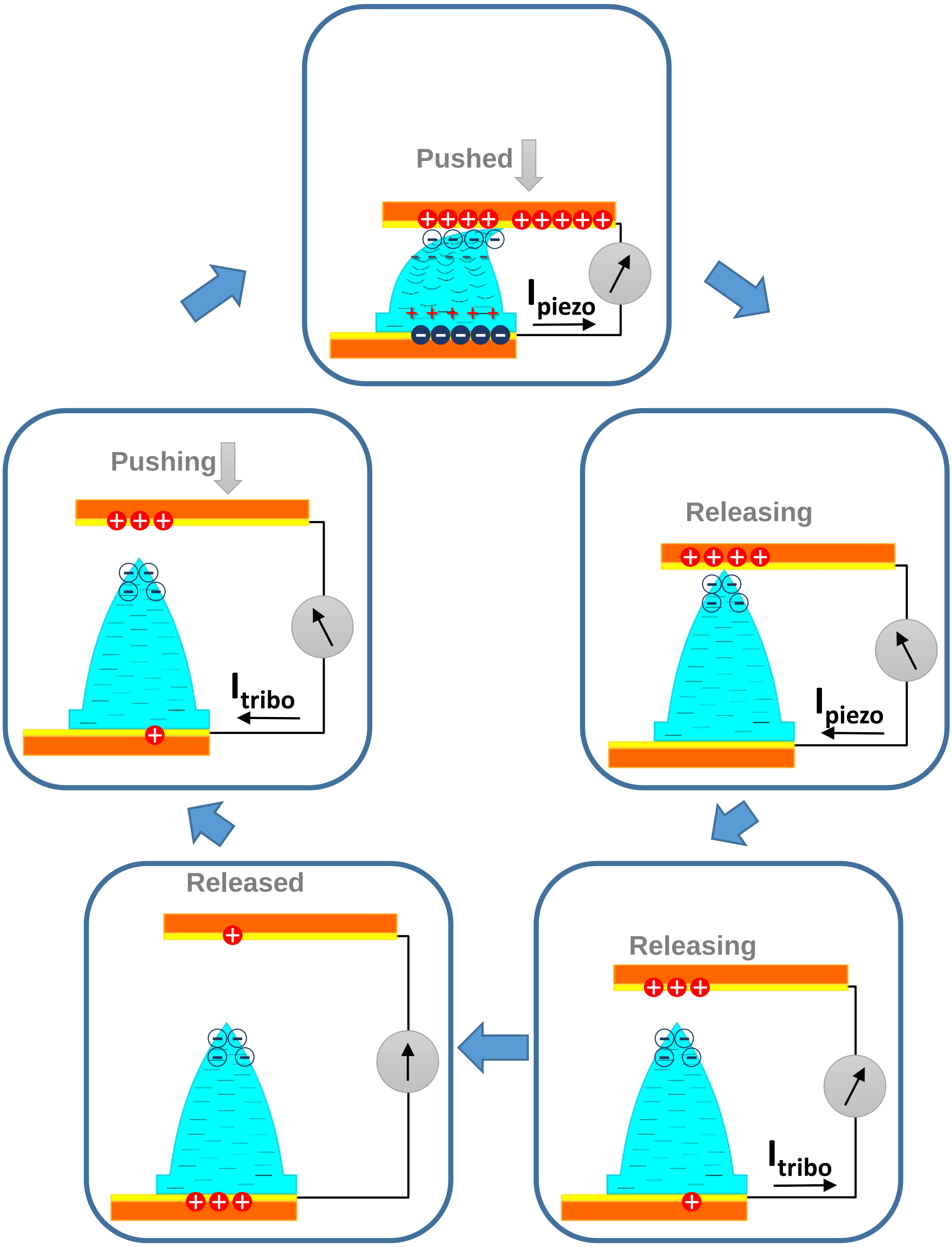

Figure S6. Proposed charge generation and displacement mechanism for both the piezoelectric and triboelectric effects in micro-structured devices. When the device is pressed, piezoelectric charges (- and +) are induced in the composite and counter charges (⊕ and ⊖) are induced in the electrodes by piezoelectric effect, which immediately generates a piezoelectric current detected by the ammeter. Negative ($\ominus$) charges are also induced by triboelectric effect in the interface between the composite’s surface, as well as positive ($\oplus$) in the top electrode. When the pressure is released until the point that the $ZnSnO_3$ nanowires are back to their original position in the composite, another piezoelectric current with the opposite direction is induced. As the pressure is released, the top electrode gets further away from the composite, which induces a charge compensation between the electrodes of the device and gives rise to a triboelectric current. When the top electrode has the maximum distance possible from the composite, the charges are in an equilibrium state and there is no current flowing through the ammeter. After this stage, a new pressure stimulus is applied to the device, approximating the top electrode to the composite and forcing the triboelectric charges in the electrodes to rearrange to balance the charges of the composite, which induces another triboelectric current with the opposite direction to flow through the ammeter. Finally, in the maximum compression state, no triboelectric current is detected, but a new piezoelectric current arises, initiating a new cycle with the same steps.

Table S2. Piezoelectric/triboelectric peak-to-peak voltage and current from the devices shown in Figure 4a and b.

Design	Peak-to-Peak Voltage (V)	Peak-to-Peak Current (μA)
Unstructured $ZnSnO_3$@PDMS	0.5 ± 0.02	0.15 ± 0.01
Micro-structured $ZnSnO_3$@PDMS (Aligned cones, gap between cones = 0 μm)	3.8 ± 0.11	0.23 ± 0.01
Micro-structured $ZnSnO_3$@PDMS (Misaligned cones, gap between cones = 0 μm)	3.5 ± 0.16	0.24 ± 0.01
Micro-structured $ZnSnO_3$@PDMS (Aligned cones, gap between cones < 100 μm)	8.7 ± 0.12	1.25 ± 0.03
Micro-structured $ZnSnO_3$@PDMS (Misaligned cones, gap between cones < 100 μm)	4.8 ± 0.15	0.41 ± 0.03

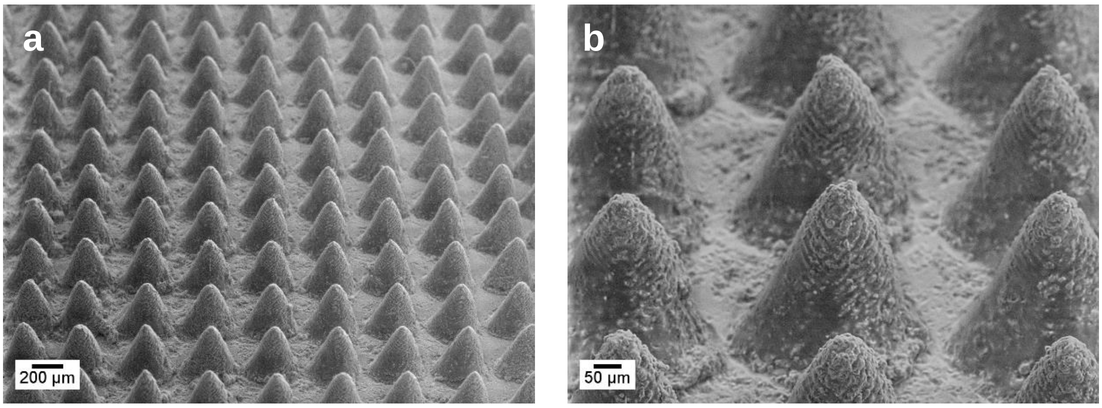

Figure S7. SEM images of $ZnSnO_3$@PDMS micro-structured films with aligned micro-cones with a gap between cones < 100 µm after the stability test (12000 cycles of pushing force). No apparent degradation of the micro-cones is seen.

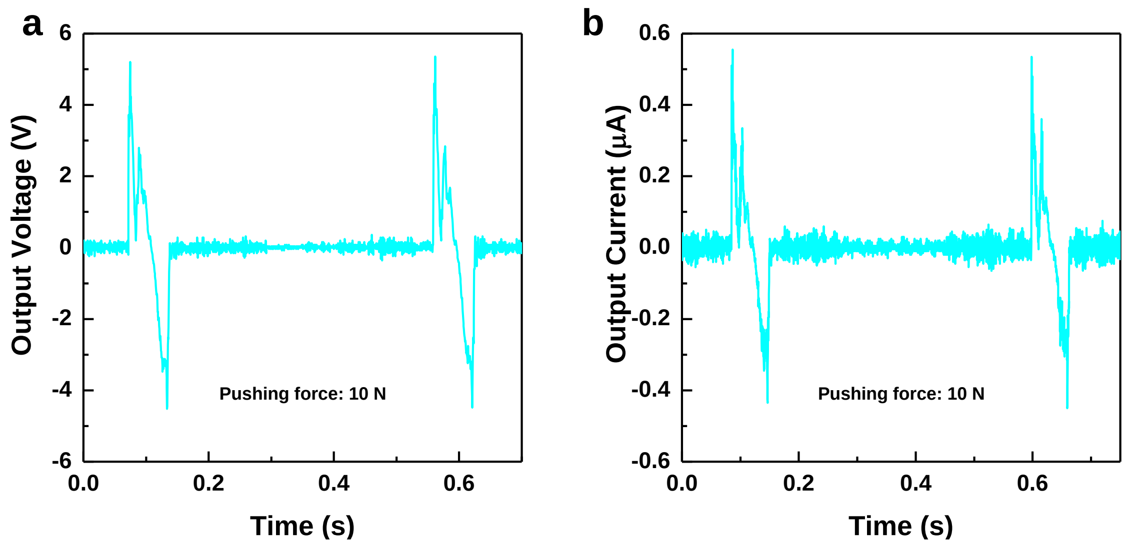

Figure S8. Output (a) voltage and (b) current generated from the $ZnSnO_3$@PDMS micro-structured films with aligned micro-cones with a gap between cones < 100 μm, one month after the initial measurements shown in Figure 4.

The I-V curves of commercial LEDs, used as practical applications of the fabricated $ZnSnO_3$ nanowires@PDMS devices, were obtained by applying voltage sweep, using a Keysight B1500A system.

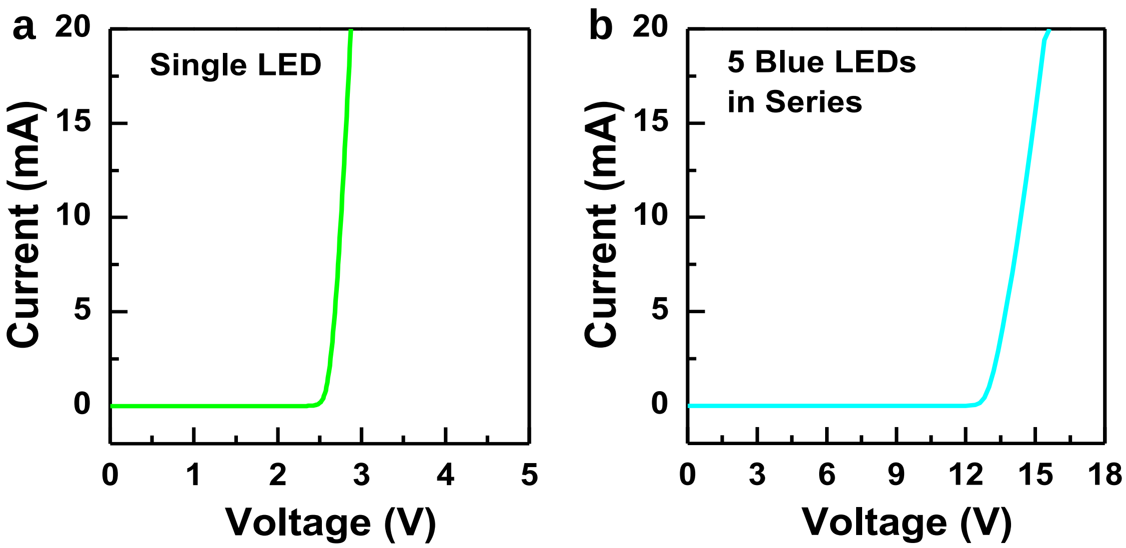

c

LEDs	Voltage (V)	Current (μA)
Single	2.3	1.56
5 in series	11.4	0.13

Figure S9. I-V curve of (a) a single (white) LED, and (b) five (blue) LEDs in series. (c) Table showing the necessary voltage and current outputs to turn on the LEDs.

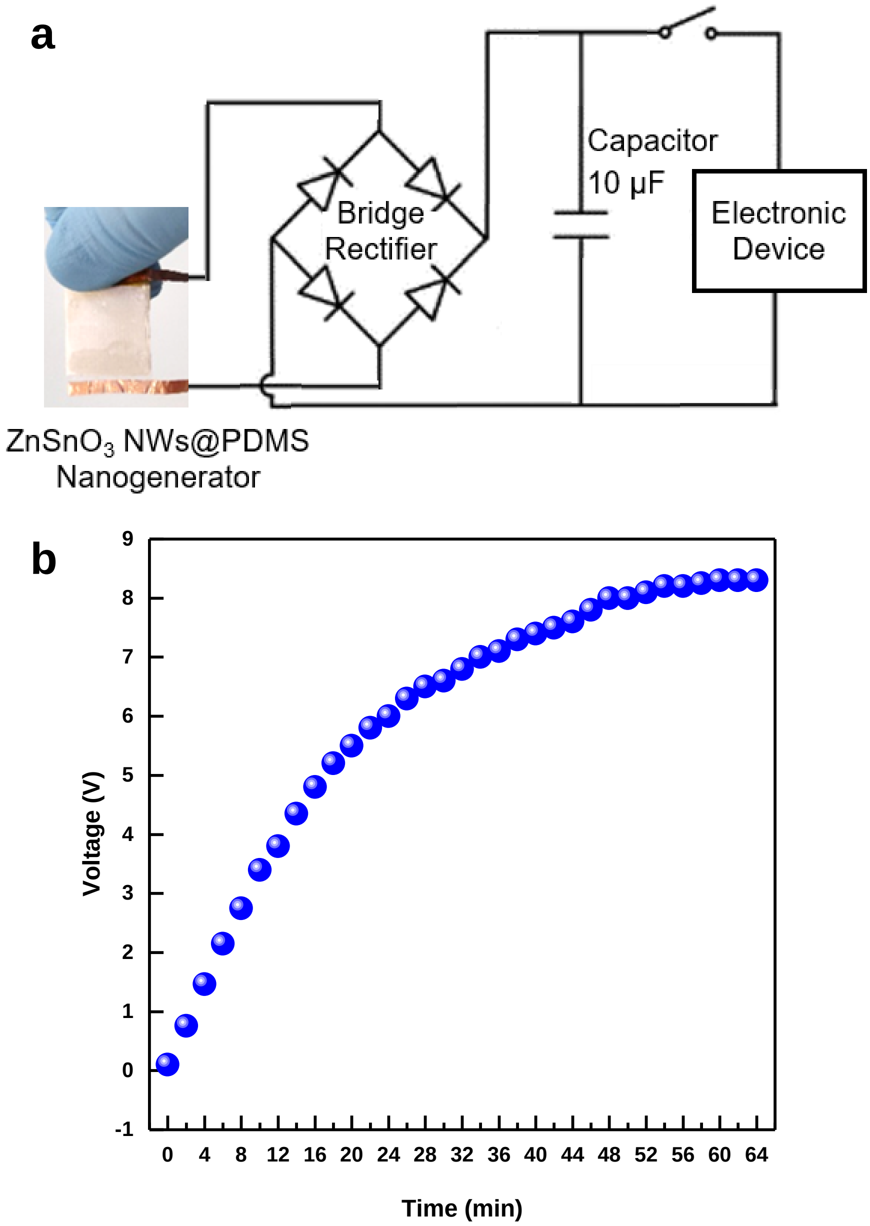

Figure S10. (a) Circuit schematic for the powering of electronic devices through the charging of a 10 µF capacitor using a micro-structured $ZnSnO_3$ NWs@PDMS nanogenerator. (b) Measured voltage in the capacitor during the charging process. Note that the multiple measurements of the capacitor voltage result in a significant voltage drop due to the discharging through the measurement probe (10 MΩ), yielding longer overall charging times.

Supplementary video 1: Home-made machine used for mechanical stimulation of the nanogenerators.

Supplementary video 2: Pressing-releasing cycles on the $ZnSnO_3$@PDMS micro-structured nanogenerator.

Supplementary video 3: Pressing-releasing cycles on the $ZnSnO_3$@PDMS unstructured nanogenerator.

Supplementary video 4: Powering a single white LED by direct connection and mechanical stimulation of the $ZnSnO_3$@PDMS micro-structured nanogenerator.

Supplementary video 5: Powering five blue LEDs by direct connection and mechanical stimulation of the $ZnSnO_3$@PDMS micro-structured nanogenerator.

Supplementary video 6: Powering small electronic devices via a 10 µF capacitor previously charged by the $ZnSnO_3$@PDMS micro-structured nanogenerator.

References

(1) Coelho, D. Solution Based Synthesis of ZnO Nanorods for Optoelectronic Applications, FCT-UNL, 2019.

(2) Ghasemian, M. B.; Lin, Q.; Adabifiroozjaei, E.; Wang, F.; Chu, D.; Wang, D. Morphology Control and Large Piezoresponse of Hydrothermally Synthesized Lead-Free Piezoelectric (Bi0.5Na0.5)TiO3 Nanofibres. *RSC Adv*. **2017**, *7* (25), 15020–15026.

(3) Shoji, I.; Kondo, T.; Kitamoto, A.; Shirane, M.; Ito, R. Absolute Scale of Second-Order Nonlinear-Optical Coefficients. *J. Opt. Soc. Am. B* **1997**, *14* (9), 2268.

(4) Liang, L.; Kang, X.; Sang, Y.; Liu, H. One-Dimensional Ferroelectric Nanostructures: Synthesis, Properties, and Applications. *Adv. Sci.* **2016**, *3* (7), 1500358.

(5) Nguyen, S. D.; Halasyamani, P. S. Synthesis, Structure, and Characterization of Two New Polar Sodium Tungsten Selenites: Na2(WO3)3(SeO3)·2H2O and Na6(W6O19)(SeO3)2. *Inorg. Chem*. **2013**, *52* (5), 2637–2647.

(6) Ke, T.-Y.; Chen, H.-A.; Sheu, H.-S.; Yeh, J.-W.; Lin, H.-N.; Lee, C.-Y.; Chiu, H.-T. Sodium Niobate Nanowire and Its Piezoelectricity. *J. Phys. Chem. C* **2008**, *112* (24), 8827–8831.

(7) Tang, H.; Zhou, Z.; Sodano, H. A. Large-Scale Synthesis of BaxSr1−xTiO3 Nanowires with Controlled Stoichiometry. *Appl. Phys. Lett*. **2014**, *104* (14), 142905.

(8) Yun, B.; Park, Y.; Lee, M.; Lee, N.; Jo, W.; Lee, S.; Jung, J. Lead-Free LiNbO3 Nanowire-Based Nanocomposite for Piezoelectric Power Generation. *Nanoscale Res. Lett*. **2014**, *9* (1), 4.

(9) Joung, M.-R.; Seo, I.-T.; Kim, J.-S.; Xu, H.; Han, G.; Kang, M.-G.; Kang, C.-Y.; Yoon, S.-J.; Nahm, S. Structural Dependence of the Piezoelectric Properties of KNbO3 Nanowires Synthesized by the Hydrothermal Method. *Acta Mater.* **2013**, *61* (10), 3703–3708.